ARCHIVES OF ACOUSTICS
**32**, 4, 923–931 (2007)

# MODELING OF TORSIONAL VIBRATION IN HARMONIC DRIVES

Ryszard LENIOWSKI

Rzeszów University of Technology
Department of Electrical Engineering and Informatics
W. Pola 2, 35-959 Rzeszów, Poland
e-mail: lery@prz-rzeszow.pl

(*received July 15, 2007; accepted October 24, 2007*)

Harmonic Drives (HD) play a considerable role in industrial applications and precise medical equipments. They offer unique features, such as high gear ratios, high torque capacities, compact geometry, zero backslash and high efficiency. However, the torsional flexibility, friction and nonlinear hysteresis lead to complex dynamic behavior of the system, which reveals as torsional vibrations. Hence, to improve the performance of new machines, the transmission compliance and internal friction mechanism must be analyzed.

This paper is concerned with precise mathematical modeling of HD. The proposed model consists of three components: hysteresis, friction and torsion flexibility. The hysteresis has been modeled as weighted combination of individual Preisach cells to form global operator, which generates adequate hysteresis curve due to measured data. Friction model includes a lubricated contact force and dynamic behavior developed by Bliman & Sorine. The last component of the HD model describes the flexspline flexibility (the flexspline is a flexible cylinder made of steel with outer teeth), that produces substantial transmission torsion. Original proposition assumes that the flexspline can be modeled as cylindrical shell FEM model ($n \times m$ degree of freedom mass-spring-damper system), based on 16 directional mesh (four nearest-stretch springs, four diagonal-shear springs and eight next-nearest neighbors, nonlinear bend spring). The flexspline is loaded on both sides by the various forces which are tangent to the flexspline surface. The friction torques has been taken into account on both sides of HD: one in the input side, another on the output side.

Simulation results show that the developed model has satisfactory features and accuracy and can be used in ongoing research to develop variant of MRAC-type controllers for vibration cancellation.

**Keywords:** vibrations, harmonic drives, mathematical modeling, computer simulations.

## 1. Introduction

In robotics, two transmitters have a great influence due to unique performance (high torque capacity, concentric geometry, lightweight, compactness, zero backslash, high efficiency): harmonic drives (HD) and tooth-belt gear (TBG). But for light-weight robots of high precision, the flexibility and nonlinearity of both type of transmitters have to be included. Proposed the accurate model of HD consists of three components: hysteresis, friction and torsion flexibility. The hysteresis has been modeled as weighted combination of individual Preisach cells to form global operator, which generates adequate hysteresis curve due to measured data. Friction model includes a lubricated contact force and dynamic behavior developed by Bliman & Sorine [3]. The last component of the HD model describes flexspline flexibility, that produces substantial transmission torsion. The cylindrical shell FEM model [1] is based on 8 directional mesh (36 stacks and 4 slices) with 4 additional “long-distance” neighbors and two kinds of force balances: tangential and radial. The TBG flexibility model includes only axial stretching and was modeled as $n$-degree of freedom mass-spring-damper system.

## 2. FEM model of harmonic drive deformations

The harmonic drive has three rotational parts. Due to differential-gearing functions, numerous reduction ratios can be achieved. In its typical configuration, the circular spline is fixed to the ground and motor drives the wave generator to produce high-torque, low-speed rotation on the flexspline. High flexibility of the flexspline is one of the inconvenient features of the HD. The goal of the modeling nonlinear dynamic of the flexspline is to derive as simple as possible mathematical model, which can predict the HD behavior with high level of accuracy. Because of complex, non-stationary surface contact between wave generator-flexpline and flexspline-circular spline, the simple torsion deformation model of rod cannot be used. Proposed solution assumes, that flexspline is modeled as FE circular cylindrical shell loaded on both sides by the various forces which are tangent to the flexspline surface (Fig. 1.).

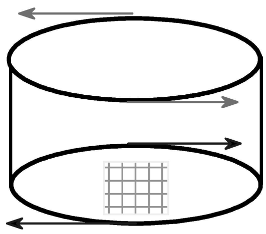

Fig. 1. Cylindrical flexspline.

The structure of mass-spring connectivity is depicted in Fig. 2a, b, c, d. Each mass of the grid is connected to its eight neighbours by the springs (four nearest-stretch springs, four diagonal-shear springs). Finally, each mass is connected to the eight next-nearest neighbours (nonlinear bend spring).

Each line segment shown in Fig. 2 moves in three-dimensional space and has reference configuration with initial length $L_0$ (see Fig. 3).

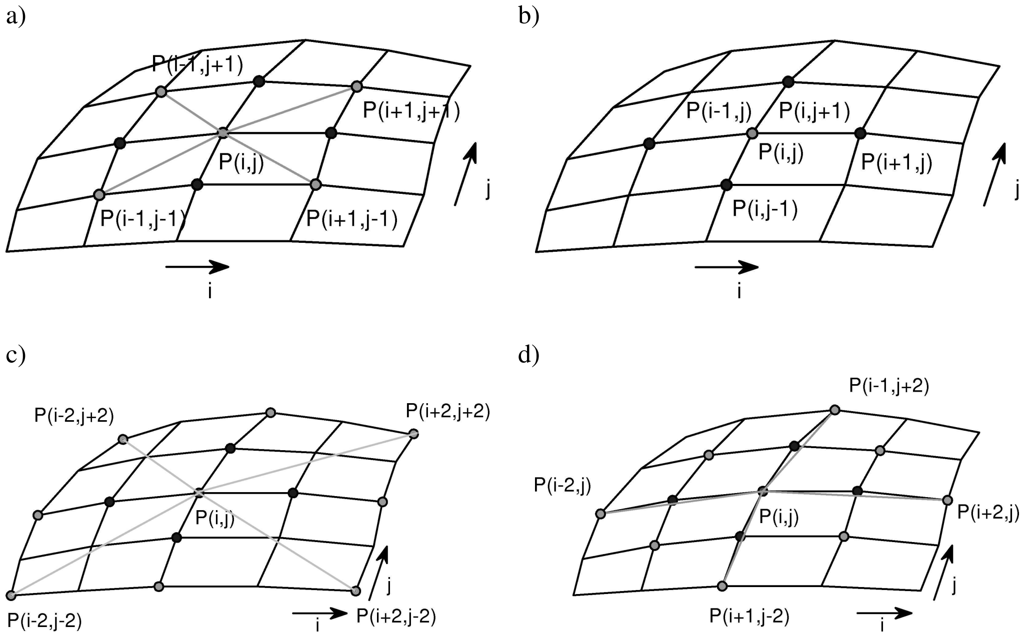


Fig. 2. FE mass-spring model connectivity, stretch springs, shear springs, bending springs.

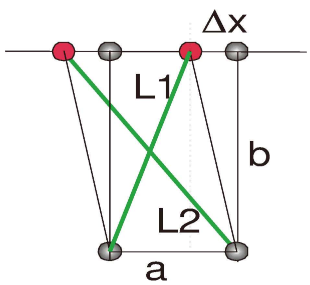


Fig. 3. Reference and current configurations of model connectivity.

For the current configuration (Fig. 3) we can calculate tangent force produced by two links:

$$F_x = F_{x1} + F_{x2} = k\left(-(L_1 - L_0)\frac{(a-\Delta x)}{L_1} + (L_2 - L_0)\frac{(a+\Delta x)}{L_2}\right), \tag{1}$$

where $L_1 = \sqrt{b^2 + (a-\Delta x)^2}$ and $L_2 = \sqrt{b^2 + (a+\Delta x)^2}$.

Static characteristic of (1) is nonlinear (Fig. 4) and is adequate to empirical data.

Let us notice (Fig. 3) that link $L_2$ is stretched for any $\Delta x$, but link $L_1$ for $a > \Delta x \geq 0$ is clamped and for $2a > \Delta x > a$ is stretched. For the another direction of the flexpline rotation the role of the links are changed themselves. To obtain 3D model several assumptions were made. Initial length of the links expresses as follows $L_0 = \sqrt{L_{x0}^2 + L_{y0}^2 + L_{z0}^2}$, where $L_{x0} = X_2(0) - X_1(0)$ and other coordinates of

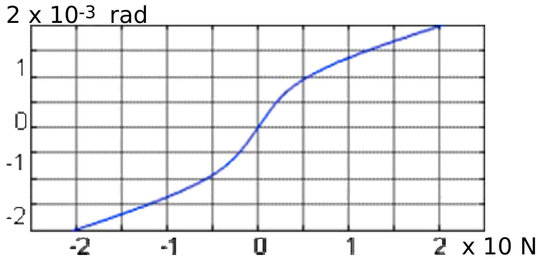


Fig. 4. Tangent force/deformation characteristic.

difference of nodes positions in the beginning are defined similarly. Actual value of $L = \sqrt{L_x^2 + L_y^2 + L_z^2}$ and its difference equals

$$\dot{L} = \frac{\mathrm{d}L}{\mathrm{d}t} = \frac{L_x}{L}\frac{\mathrm{d}L_x}{\mathrm{d}t} + \frac{L_y}{L}\frac{\mathrm{d}L_y}{\mathrm{d}t} + \frac{L_z}{L}\frac{\mathrm{d}L_z}{\mathrm{d}t} = \widehat{\mathbf{L}}^{\mathrm{T}}\dot{\mathbf{u}}_L, \tag{2}$$

where

$$\widehat{\mathbf{L}}^{\mathrm{T}} = [L_x/L \;\; L_y/L \;\; L_z/L]^{\mathrm{T}} \tag{3}$$

describes the cosine vectors and

$$\mathbf{u}_L = \mathbf{L} - \mathbf{L}_0 \tag{4}$$

is introduced to simplify the kinematic equations. The second derivative of the spring length with respect to time is

$$\ddot{L} = \dot{\mathbf{u}}_L^{\mathrm{T}}\mathbf{H}\dot{\mathbf{u}}_L + \widehat{\mathbf{L}}^{\mathrm{T}}\ddot{\mathbf{u}}_L\,, \tag{5}$$

where matrix $\mathbf{H} = \dfrac{1}{L}\left(\mathbf{I} - \widehat{\mathbf{L}}\widehat{\overline{\mathbf{L}}}^{\mathrm{T}}\right)$. Having all necessary kinematic parameters, we can use Lagrange principle to derive PDE of motion in iterative matrix form

$$\ddot{q}_{ij}(k) = m_{ij}^{-1}\left(F_{ij}(i) - k\sum_{m=1}^{16}(L_m - L_{0m})\widehat{\mathbf{L}} - \mu\sum_{m=1}^{16}\dot{L}\widehat{\mathbf{L}}^{\mathrm{T}}\widehat{\mathbf{L}}\right). \tag{6}$$

Variable $\ddot{q}_{ij}$ denotes the resultant acceleration of $i$-th node, $m_{ij}$ is a node mass, $F_{ij}$ – external forces of the nodes. Two of the last elements describes forces and damping interactions between sixteen neighbours nodes. The gravity forces has been neglected for HD model. Software component of FEM harmonic drive model is based on Eq. (6). Additional dependences describes friction and hysteresis phenomena.

## 3. Model of the friction

The classical models consist of several elements, which separately describe aspects of friction. All of them assume that friction opposes motion and can be expressed by simple analytical functions. These are called classic models (see Table 1).

**Table 1.** Classic models of friction.

| Name of model | Model |
|---|---|
| Coulomb | $F = F_C\,\mathrm{sign}(v)$ |
| Viscous | $F = F_V v$ |
| Static | $F = \begin{cases} F_e & \text{if } v = 0 \text{ and } \lvert F_e\rvert < F_s \\ F_s\,\mathrm{sign}(F_e) & \text{if } v = 0 \text{ and } \lvert F_e\rvert \geq F_s \end{cases}$ |
| Stribeck effect | $F = (F_S - F_C)e^{-\lvert v/v_s\rvert^{\delta_s}}$ |
| Karnnopp | $F = \begin{cases} F(v) & \lvert v\rvert \geq DV \\ F(F_e) & \lvert v\rvert < DV \end{cases}$ |
| Armstrong | $F = \begin{cases} F(x) & \text{static} \\ F(v,t) & \text{dynamic} \end{cases} \quad F(x) = \sigma_0 x$ <br> $F(v,t) = \left(F_C + F_S(\gamma, t_d)\dfrac{1}{1 + (v(t-\tau_l)/v_s)^2}\right)\mathrm{sign}(v) + F_V v$ <br> $F_S(\gamma, t_d) = F_{S,\propto} + \left(F_{S,\infty} - F_{S,\propto}\dfrac{t_d}{t_d + \gamma}\right)$ |

For modern control methods design, the classic model of friction is not satisfactory. Dynamic friction models have substantial influence, when high precision of motion is required. The essential advance friction models are: Dahl, Bristle, Heassing, Bliman&Sorine, Lubricated Contact and LuGre [3]. Each of mentioned models can be used to implement friction compensators, but for gear simulation the Bliman&Sorine model seems most adequate. It assumes that the magnitude of the friction depends only on velocity and variable $s$ defined as follows

$$s = \int_0^t \lvert v(\tau)\rvert\,\mathrm{d}\tau\,. \tag{7}$$

Having $s$ defined, the friction model simplifies to linear state system (8). The "control" variable $v_s$ is equal $v_s = \mathrm{sign}(v(t))$.

$$\begin{aligned} \frac{\mathrm{d}x_s}{\mathrm{d}s} &= Ax_s + Bv_s\,, \\ F &= Cx_s\,. \end{aligned} \tag{8}$$

There are a great number of configuration possibilities, due to the model order and the set of matrixes coefficients. It seems that based on the Bliman&Sorine model and hysteresis operator described in the next paragraph some useful transfer functions for mathematical modeling of robot transmitter parts can be developed.

## 4. Model of the hysteresis

Hysteresis is the third important attribute of precision robot servo system. It is well-known, that harmonic drive introduces rest hysteresis to the system. Engineering data for harmonic drive gears include complicated-shape characteristic of hysteresis (see Fig. 5). Moreover, some of accuracy parameters introduces additional disturbances, for example repeatability, which describes the position difference measured during repeated movement to the same desired position from the same direction.

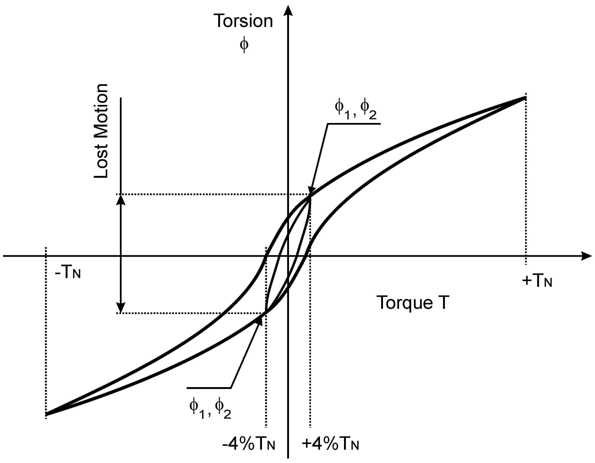


Fig. 5. Hysteresis curve.

Hysteresis phenomenon is effectively modeled using Preisach operator [3]. It assumes, that the hysteresis characteristics can be obtained as a combination of individual relay elements (called Preisach cells) in order to form a global operator. Preisach hysteron and the scheme of discretized operator are shown in the Fig. 6.

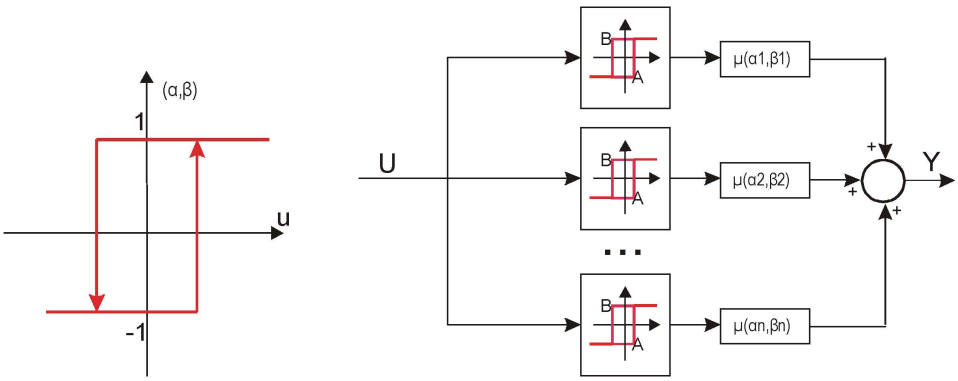


Fig. 6. Relay characteristic and hysteresis, discrete model.

Equivalent mathematical formula is given by

$$y(t) \cong \sum_{i=1}^{n} \mu_i(\alpha, \beta)\gamma_{(\alpha,\beta),i}(u). \tag{9}$$

The values of pair $(\alpha, \beta)$ and the weight coefficients $\mu(\alpha, \beta)$ are tuned to the individual characteristic of a HD model. However, the Preisach model has a intrinsic disadvantage: the hysteresis function is non-differentiable.

## 5. Software components and simulations results

The software of harmonic drives consists of three components and corresponding test suites. All of the components belong to the flexible light-weight robot software library – a collection of modules and functions which are necessary for the light-weight robots simulation. The library supports the arm deformations models, flexible gear boxes (including presented friction and hysteresis models), transmitter link models, PZT actuator model and sensor models (position, acceleration, vision and strain gauges).

From mathematical modeling point of view, harmonic drive is a two-input two-output system (Fig. 7). The input signals are wave generator angular position (or velocity and load flexpline torque), while outputs are angular flexpline position (or velocity, and wave generator torque which is motor load torque). It should be not forgotten that the input to the system is the motor rotation which is transmitted through the wave generator by a reduction mechanism to the flexspline.


Fig. 7. HD model.

The inside structure of harmonic drive (Fig. 8) includes four function blocks. It was designed to form the functions into sequence adequate to the gear construction and energy transmissions and dissipations.

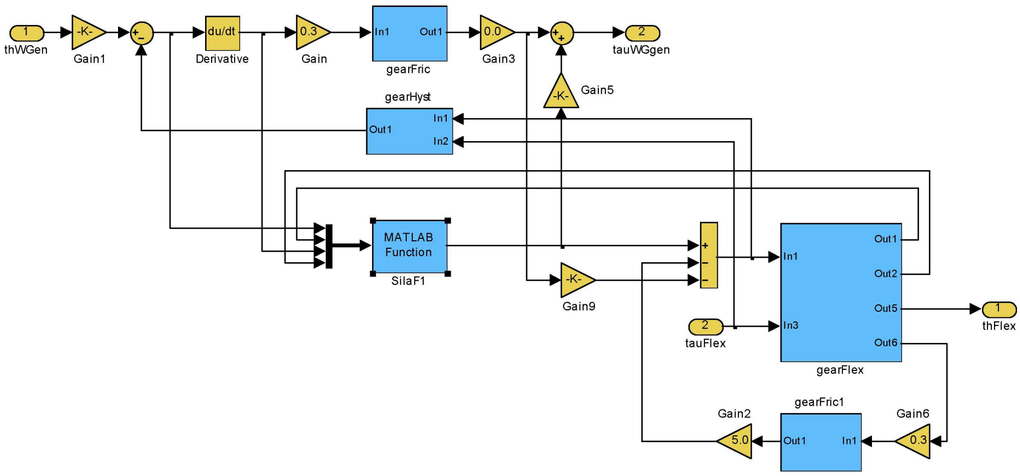


Fig. 8. The inside structure of HD.

The *gearHD* computes the flexibility model of gear box, utilizing Eq. (6).

The friction block *gearFric* is the same in wave generator and flexpline. The Bliman&Sorine model (see details on Sec. 3) was used, to have time, position and velocity dependent steady-state friction subsystem (7, 8). The hysteresis block *gearHyst* is complementary component of friction and torsional flexibility models.

The software project has been developed in Visual C++ (*MSDV*) and *OpenGL* (3D graphics library). Most of modules have been translated to *Matlab* environment.

To validate the proposed harmonic drive model, a simulation has been performed for different cases. Figure 9a, b, c shows the results of transmitted position angle across the flexpline. The repeating step as the wave generator reference signal and constant -50 Nm load torque form the desired input of the HD.

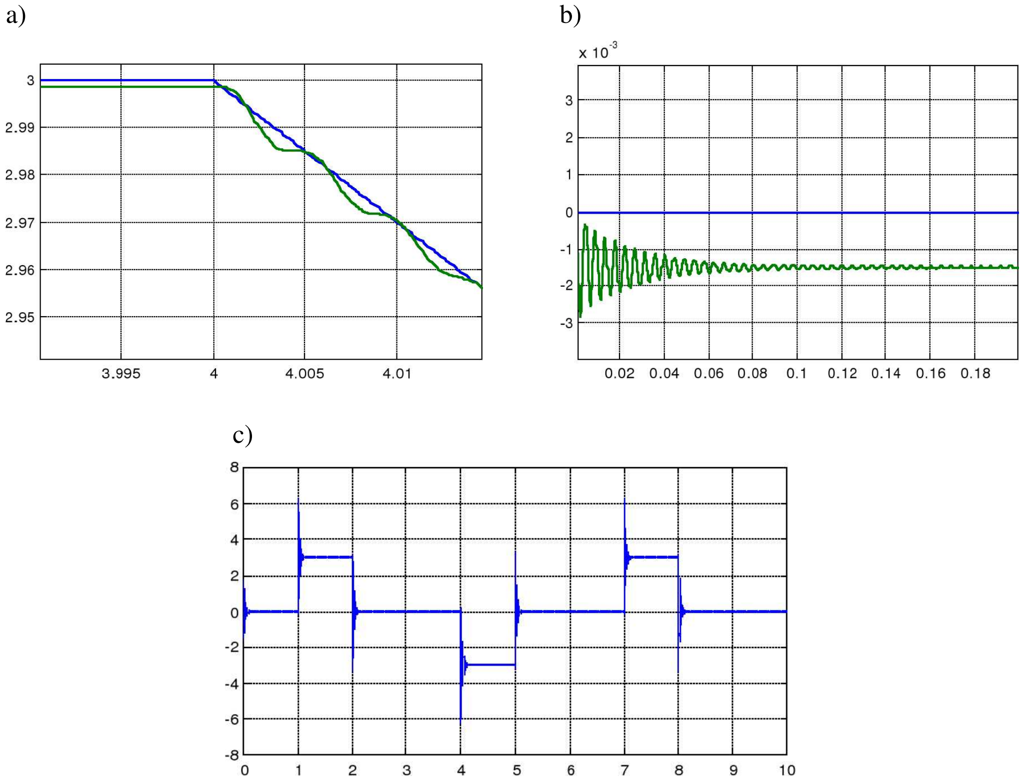


Fig. 9. a, b) Position angle of wave generator and flexpline angle, c) the flexpline velocity. Horizontal axis – time in seconds (0.1 ms sampling time), vertical axis – radians $\times 1e{-3}$, (a, b), radian/s (c).

Carefully observing Fig. 9b, it can be noticed that there is a subtle difference between referenced position angle and the result flexpline. The computed flexpline position angle has small damped oscillation, when reference signals are quickly changed. The other visible effect is a small steady error for constant flexpline load, a result of equilibrium between HD stiffness torque and load. It is remarkable that the developed model has satisfactory features and accuracy and can be used in ongoing research to develop variant of MRAC-type controllers for vibration cancellation. However, computation complexity is too high and must be reduced to real-time appliances.

## 6. Conclusions

The model has been verified comparing the simulated behavior of the system to the experimental result published by Harmonic Drive AG and GHORBEL [4]. An accurate match in the result indicates the reliability of the model for wide operating conditions. This proposed model is utilized for model reference control purposes in a new generation light-weight robots ongoing research.

## Acknowledgment

This work was supported by Grant N514 013 31/3317 from the Ministry of Science and Higher Education of Poland.

## References

[1] FELIPPA C., *Customizing the Mass and Geometric Stiffness of Plane Thin Beam Elements by Fourier Methods*, Rapport of College of Engineering, University of Colorado, 2000.

[2] TAN X., BARAS J., KRISHANAPRASAD P. S., *Control of hysteresis in smart actuators with application to micro-positioning*, Systems & Control Letters, **54**, 483–492 (2005).

[3] CANUDAS DE WIT C., OLSSON H., ASTROM K. J., LISCHINSKY P., *Adaptive friction compensation with partially known dynamic friction model*, Int. J. of Adap. Contr. and Sig. Processing, No. 11, 1997.

[4] DHAOUADI R., GHORBEL F., *Modeling and Analysis of Hysteresis in Harmonic Drive Gears*, Sys. Analysis Model Simul., 1, 1–14 (2003).